

Reactive Power Control of Permanent-Magnet Synchronous Wind Generator With Matrix Converter

Hossein Hojabri, Hossein Mokhtari, *Member, IEEE*, and Liuchen Chang, *Senior Member, IEEE*

Abstract—In this paper, the reactive power control of a variable-speed permanent-magnet synchronous wind generator with a matrix converter at the grid side is improved. A generalized modulation technique based on singular value decomposition of the modulation matrix is used to model different modulation techniques and investigate their corresponding input reactive power capability. Based on this modulation technique, a new control method is proposed for the matrix converter which uses active and reactive parts of the generator current to increase the control capability of the grid-side reactive current compared to conventional modulation methods. A new control structure is also proposed which can control the matrix converter and generator reactive current to improve the grid-side maximum achievable reactive power for all wind speeds and power conditions. Simulation results prove the performance of the proposed system for different generator output powers.

Index Terms—Matrix converter, permanent-magnet synchronous generator (PMSG), reactive power control, singular value decomposition (SVD) modulation, variable-speed wind generator.

I. INTRODUCTION

A MATRIX converter is a direct ac/ac frequency converter which does not require any energy storage element. Lack of bulky reactive components in the structure of this all silicon-made converter results in reduced size and improved reliability compared to conventional multistage ac/dc/ac frequency converters. Fabrication of low-cost and high-power switches and a variety of high-speed and high-performance digital signal processors (DSPs) have almost solved some of the matrix converter drawbacks, such as complicated modulation, four-step switching process of bidirectional switches, and the use of a large number of switches [1]. Therefore, its superior benefits, such as sinusoidal output voltage and input current, controllable input power factor, high reliability, as well as a small and packed structure make it a suitable alternative to back-to-back converters.

One of the recent applications of matrix converters is the grid connection of variable-speed wind generators [2]–[14]. Vari-

able-speed permanent-magnet synchronous (PMS) wind generators are used in low-power applications. The use of a matrix converter with a multipole PMSG leads to a gearless, compact, and reliable structure with little maintenance which is superior for low-power microgrids, home, and local applications [13], [15]–[17].

The wind generator frequency converter should control the generator-side quantities, such as generator torque and speed, to achieve maximum power from the wind turbine, and the grid-side quantities such as grid-side reactive power and voltage to improve the system stability and power quality (PQ) [17]–[19]. Unlike conventional back-to-back converters in which a huge dc-link capacitor makes the control of the generator and grid-side converters nearly independent [20], a matrix converter controls the generator and grid-side quantities simultaneously. Therefore, the grid-side reactive power of a matrix converter is limited by the converter voltage gain and the generator-side active or reactive power [21].

One necessary feature for all generators and distributed generators (DGs) connecting to a grid or a microgrid is the reactive power control capability. The generator reactive power can be used to control the grid or microgrid voltage or compensate local loads reactive power in either a grid-connected or an islanded mode of operation [19], [20]. In this paper, the grid-side reactive power capability and control of a PMS wind generator with a matrix converter is improved. For this purpose, in Section II, a brief study of a matrix converter and its singular value decomposition (SVD) modulation technique, which is a generalized modulation method with more relaxed constraints compared to similar modulation methods is presented.

In Section III, the SVD modulation technique is used to model different modulation techniques and study the reactive power capability of a matrix converter. It is shown that in some modulation techniques, such as Alesina and Venturini, the grid-side reactive current is synthesized only by the reactive part of the generator-side current. In other modulation techniques, such as indirect methods or direct and indirect space vector modulation (SVM) methods, the grid-side reactive current is synthesized only by the active part of the generator-side current. To increase the matrix converter reactive current gain, the SVD modulation technique is used such that both active and reactive parts of the generator-side current can contribute to the grid-side reactive current.

It is shown in Section IV that the generator free reactive power capacity can be used to increase the grid-side reactive power. A new control structure is also proposed which can control the generator and matrix converter reactive power to increase the controllability of the grid-side reactive power at any

Manuscript received April 13, 2011; revised April 13, 2012; accepted November 09, 2012. Date of publication December 13, 2012; date of current version March 21, 2013. Paper no. TPWRD-00294-2011.

H. Hojabri and H. Mokhtari are with the Centers of Excellence in Power System Management and Control, Department of Electrical Engineering, Sharif University of Technology, Tehran 11365–9363, Iran (e-mail: hhojabri@ee.sharif.edu; mokhtari@sharif.edu).

L. Chang is with the Department of Electrical and Computer Engineering, University of New Brunswick, Fredericton, NB E3B 5A3 Canada (e-mail: LChang@unb.ca).

Digital Object Identifier 10.1109/TPWRD.2012.2229721

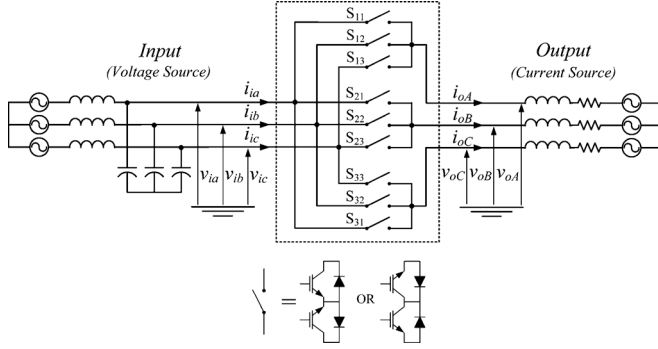


Fig. 1. Typical three-phase matrix converter schematic.

wind speed and power. The proposed control structure is simulated with a simple adaptive controller (SAC) on a gearless multipole variable-speed PMS wind generator, and the results are presented to verify its performance under different operating conditions. The simulations are performed using PSCAD/EMTDC software.

II. MATRIX CONVERTER

Fig. 1 shows a typical three-phase matrix converter. In a matrix converter, the input and output phases are related to each other by a matrix of bidirectional switches such that it is possible to connect any phase at the input to any phase at the output. Therefore, the controllable output voltage is synthesized from discontinuous parts of the input voltage source, and the input current is synthesized from discontinuous parts of the output current source or

$$\begin{aligned}
 V_{o,ABC} &= \mathbf{S}V_{i,abc} \\
 I_{i,abc} &= \mathbf{S}^T I_{o,ABC} \\
 \mathbf{S} &= \begin{pmatrix} s_{11} & s_{12} & s_{13} \\ s_{21} & s_{22} & s_{23} \\ s_{31} & s_{32} & s_{33} \end{pmatrix} \\
 \begin{cases} s_{kj} \in \{0, 1\} \\ s_{k1} + s_{k2} + s_{k3} = 1 \end{cases} & \quad k, j = 1, 2, 3 \\
 V_{i,abc} &= \begin{pmatrix} v_{ia} \\ v_{ib} \\ v_{ic} \end{pmatrix}, \quad I_{i,abc} = \begin{pmatrix} i_{ia} \\ i_{ib} \\ i_{ic} \end{pmatrix} \\
 V_{o,ABC} &= \begin{pmatrix} v_{oA} \\ v_{oB} \\ v_{oC} \end{pmatrix}, \quad I_{o,ABC} = \begin{pmatrix} i_{oA} \\ i_{oB} \\ i_{oC} \end{pmatrix} \quad (1)
 \end{aligned}$$

where v_{oj} and i_{oj} ($j = A, B, C$) are the output phase voltages and currents, respectively; v_{ij} and i_{ij} ($j = a, b, c$) are the input phase voltages and currents; and s_{kj} is the switching function of switch kj .

Lack of an energy storage component in the structure of a matrix converter leads to an equality between the input–output active power, i.e.,

$$p_i = V_{i,abc}^T \cdot I_{i,abc} = V_{o,ABC}^T \cdot I_{o,ABC} = p_o. \quad (2)$$

A. SVD Modulation Technique

Different modulation techniques are proposed for a matrix converter in the literature [21]–[23]. A more complete modu-

lation technique based on SVD decomposition of a modulation matrix is proposed in [24]. Other modulation methods of a matrix converter can be deduced from this SVD modulation technique. The technique proposed in [24] has more relaxed constraints compared to other methods.

The SVD modulation method is a duty cycle method in which the modulation matrix \mathbf{M} , which is defined in (3), is directly constructed from the known input voltage and output current and desired output voltage and input current, i.e.,

$$\begin{aligned}
 \mathbf{M} &= \text{Ave}\{\mathbf{S}\} = \begin{pmatrix} m_{11} & m_{12} & m_{13} \\ m_{21} & m_{22} & m_{23} \\ m_{31} & m_{32} & m_{33} \end{pmatrix} \\
 \begin{cases} 0 \leq m_{kj} \leq 1 \\ m_{k1} + m_{k2} + m_{k3} = 1 \end{cases} & \quad k, j = 1, 2, 3 \quad (3)
 \end{aligned}$$

where m_{kj} is the average of s_{kj} over a switching period.

To represent the input and output voltages and currents in space vector forms, all quantities of the input and output of the matrix converter are transferred from the abc reference frame to the $\alpha\beta 0$ reference frame by the modified Clarke transformation of (4). Therefore, the new modulation matrix $\mathbf{M}_{\alpha\beta 0}$ is obtained as

$$\begin{aligned}
 V_{o,\alpha\beta 0} &= \mathbf{M}_{\alpha\beta 0} V_{i,\alpha\beta 0} \\
 I_{i,\alpha\beta 0} &= \mathbf{M}_{\alpha\beta 0}^T I_{o,\alpha\beta 0} \\
 \mathbf{M}_{\alpha\beta 0} &= \mathbf{K} \mathbf{M}_{abc} \mathbf{K}^T \\
 \mathbf{K} &= \sqrt{\frac{2}{3}} \begin{pmatrix} 1 & -\frac{1}{2} & -\frac{1}{2} \\ 0 & \frac{\sqrt{3}}{2} & -\frac{\sqrt{3}}{2} \\ \frac{1}{\sqrt{2}} & \frac{1}{\sqrt{2}} & \frac{1}{\sqrt{2}} \end{pmatrix} \\
 \mathbf{K}^{-1} &= \mathbf{K}^T \text{ OR } \mathbf{K} \mathbf{K}^T = \mathbf{I}. \quad (4)
 \end{aligned}$$

The last equality means that matrix \mathbf{K} is a unitary matrix or its transpose is equal to its inverse. Considering the condition set by (3) and using (4), the following basic form for the $\mathbf{M}_{\alpha\beta 0}$ is obtained:

$$\begin{aligned}
 \mathbf{M}_{\alpha\beta 0} &= \mathbf{K} \mathbf{M}_{abc} \mathbf{K}^T = \begin{pmatrix} g_{11} & g_{12} & 0 \\ g_{21} & g_{22} & 0 \\ c'_1 & c'_2 & 1 \end{pmatrix} \\
 &= \begin{pmatrix} \mathbf{M}_{\alpha\beta 2 \times 2} & \mathbf{0} \\ \mathbf{0} & 0 \end{pmatrix} + \underbrace{\begin{pmatrix} \mathbf{0} & \mathbf{0} \\ \mathbf{C}'_{1 \times 2} & 1 \end{pmatrix}}_{\mathbf{M}_0} \quad (5)
 \end{aligned}$$

where $\mathbf{M}_{\alpha\beta}$ generates $V_{o,\alpha\beta}$ and $I_{i,\alpha\beta}$ from $V_{i,\alpha\beta}$ and $I_{o,\alpha\beta}$, and \mathbf{M}_0 generates $V_{o,0}$ and $I_{i,0}$ from $V_{i,\alpha\beta 0}$ and $I_{o,\alpha\beta 0}$, respectively.

Since, in a three-phase three-wire system, no zero-sequence current can flow, the zero-sequence voltage can be added to the output phase voltages to increase the flexibility of the control logic. Therefore, in all modulation methods, the main effort is devoted to selecting suitable $\mathbf{M}_{\alpha\beta}$ in (6) to control the output voltage and input current and a suitable \mathbf{M}_0 to increase the operating range of the matrix converter, i.e.,

$$\begin{aligned}
 \begin{pmatrix} v_{o\alpha} \\ v_{o\beta} \end{pmatrix} &= \begin{pmatrix} g_{11} & g_{12} \\ g_{21} & g_{22} \end{pmatrix} \begin{pmatrix} v_{i\alpha} \\ v_{i\beta} \end{pmatrix} \\
 \begin{pmatrix} i_{i\alpha} \\ i_{i\beta} \end{pmatrix} &= \begin{pmatrix} g_{11} & g_{12} \\ g_{21} & g_{22} \end{pmatrix}^T \begin{pmatrix} i_{o\alpha} \\ i_{o\beta} \end{pmatrix}. \quad (6)
 \end{aligned}$$

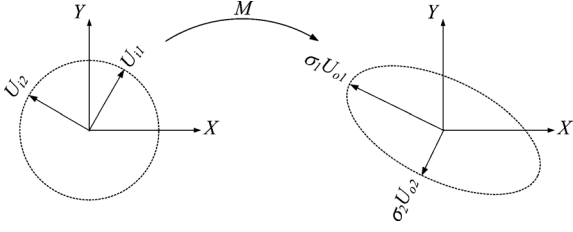
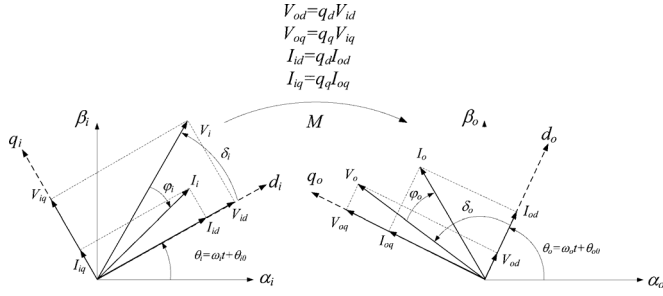


Fig. 2. Concept of the SVD of a matrix.

Fig. 3. SVD of $\mathbf{M}_{\alpha\beta}$.

$\mathbf{M}_{\alpha\beta}$ maps $V_{i,\alpha\beta}$ from the input $\alpha\beta$ space onto $V_{o,\alpha\beta}$ in the output $\alpha\beta$ space and $\mathbf{M}_{\alpha\beta}^T$ maps $I_{o,\alpha\beta}$ from the output $\alpha\beta$ space onto $I_{i,\alpha\beta}$ in the input $\alpha\beta$ space. Each matrix can be decomposed into a product of three matrices as shown in (7) which is called SVD of a matrix [25]

$$\begin{aligned} \mathbf{M} &= \mathbf{U}_o \mathbf{\Sigma} \mathbf{U}_i^* \\ \mathbf{\Sigma} &= \begin{pmatrix} \sigma_1 & 0 \\ 0 & \sigma_2 \end{pmatrix}, \begin{cases} \mathbf{U}_{o,2 \times 2} = \begin{pmatrix} U_{o1,2 \times 1} & U_{o2,2 \times 1} \end{pmatrix} \\ \mathbf{U}_{i,2 \times 2} = \begin{pmatrix} U_{i1,2 \times 1} & U_{i2,2 \times 1} \end{pmatrix} \end{cases} \\ \mathbf{U}_i \mathbf{U}_i^* &= \mathbf{U}_o \mathbf{U}_o^* = \mathbf{I} \end{aligned} \quad (7)$$

where \mathbf{U}_i and \mathbf{U}_o are unitary matrices meaning that their columns are orthonormal vectors, and the $*$ operator is conjugate transpose. σ_1 and σ_2 are the gains of matrix \mathbf{M} in the direction of U_{i1} and U_{i2} .

As Fig. 2 depicts, the SVD of a matrix means that this matrix will transform the vectors in the direction of $U_{i1,2 \times 1}$ toward the direction of $U_{o1,2 \times 1}$ by a gain of σ_1 and vectors in the direction of $U_{i2,2 \times 1}$ toward the direction of $U_{o2,2 \times 1}$ by a gain of σ_2 .

As presented in Fig. 3, $\mathbf{M}_{\alpha\beta}$ also has an SVD decomposition where $U_{i1,2 \times 1}$ and $U_{i2,2 \times 1}$ are orthonormal vectors rotating at a speed equal to the input frequency (i.e., U_{id} and U_{iq} , and $U_{o1,2 \times 1}$ and $U_{o2,2 \times 1}$ are orthonormal vectors rotating at the output frequency, that is, U_{od} and U_{oq}).

$$\begin{aligned} \begin{pmatrix} g_{11} & g_{12} \\ g_{21} & g_{22} \end{pmatrix} &= \begin{pmatrix} U_{od} & U_{oq} \end{pmatrix} \begin{pmatrix} q_d & 0 \\ 0 & q_q \end{pmatrix} \begin{pmatrix} U_{id} & U_{iq} \end{pmatrix} \\ &= \begin{pmatrix} \cos \theta_o & -\sin \theta_o \\ \sin \theta_o & \cos \theta_o \end{pmatrix} \begin{pmatrix} q_d & 0 \\ 0 & q_q \end{pmatrix} \\ &\quad \times \begin{pmatrix} \cos \theta_i & -\sin \theta_i \\ \sin \theta_i & \cos \theta_i \end{pmatrix}^T. \end{aligned} \quad (8)$$

By substituting (8) into (5), \mathbf{M}_{abc} is obtained as

$$\begin{aligned} \mathbf{M}_{abc} &= \mathbf{K}^T \mathbf{M}_{\alpha\beta} \mathbf{K} = \mathbf{K}^T \mathbf{M}_{\alpha\beta} \mathbf{K} + \mathbf{K}^T \mathbf{M}_0 \mathbf{K} \\ &= \mathbf{M}_{abc,\alpha\beta} + \mathbf{M}_{abc,0} \\ &= \mathbf{P}(\theta_o)^T \underbrace{\begin{pmatrix} q_d & 0 \\ 0 & q_q \end{pmatrix}}_{\mathbf{M}_{dq}} \mathbf{P}(\theta_i) + \mathbf{M}_{abc,0} \\ \mathbf{P}(\theta) &= \sqrt{\frac{2}{3}} \begin{pmatrix} \cos \theta & \cos(\theta - \frac{2\pi}{3}) & \cos(\theta + \frac{2\pi}{3}) \\ -\sin \theta & -\sin(\theta - \frac{2\pi}{3}) & -\sin(\theta + \frac{2\pi}{3}) \end{pmatrix} \end{aligned} \quad (9)$$

where $\mathbf{P}(\theta)$ is the modified Park transformation matrix.

It can be proved that if the following limitation on q_d and q_q is held, there exists a $\mathbf{M}_{abc,0}$ matrix for which the condition of (3) is correct [24]. Therefore

$$\begin{aligned} &\left. \begin{aligned} |q_d| + |q_q| \leq 1 \\ \max\{|q_d|, |q_q|\} \leq \frac{\sqrt{3}}{2} \end{aligned} \right\} \Rightarrow \\ &\begin{cases} 0 \leq m_{kj} \leq 1 \\ m_{k1} + m_{k2} + m_{k3} = 1, \quad k, j = 1, 2, 3. \end{cases} \end{aligned} \quad (10)$$

There may be many solutions for matrix $\mathbf{M}_{abc,0}$; however, the following solution requires simple calculations [24]:

$$\begin{aligned} \mathbf{M}_{abc,0} &= \begin{pmatrix} c_1 & c_2 & c_3 \\ c_1 & c_2 & c_3 \\ c_1 & c_2 & c_3 \end{pmatrix} \\ c_k &= -\min_i \{ \mathbf{M}_{abc,\alpha\beta}(\mathbf{i}, \mathbf{k}) \} \\ &\quad + \left\{ 1 + \sum_j \min_i \{ \mathbf{M}_{abc,\alpha\beta}(\mathbf{i}, \mathbf{j}) \} \right\} \\ &\quad \cdot \frac{1 - \max_i \{ \mathbf{M}_{abc,\alpha\beta}(\mathbf{i}, \mathbf{k}) \} + \min_i \{ \mathbf{M}_{abc,\alpha\beta}(\mathbf{i}, \mathbf{k}) \}}{3 - \sum_j \max_i \{ \mathbf{M}_{abc,\alpha\beta}(\mathbf{i}, \mathbf{j}) \} + \sum_j \min_i \{ \mathbf{M}_{abc,\alpha\beta}(\mathbf{i}, \mathbf{j}) \}}. \end{aligned} \quad (11)$$

The constraint obtained in (10) is an inherent constraint of a matrix converter which is more relaxed than the constraint of conventional modulation methods. Therefore, the use of the SVD modulation technique can improve the performance of a matrix converter when the input reactive power control is needed [23], [24].

All of the existing modulation methods can be deduced from this simple and general method by choosing suitable q_d , q_q , θ_i , and θ_o . On the other hand, (9) shows that if the input and output quantities are transferred onto their corresponding synchronous reference frames, the SVD modulation matrix becomes a simple, constant, and time-invariant matrix (i.e., \mathbf{M}_{dq}). Therefore, as shown in Fig. 4, the SVD modulation technique models the matrix converter as a dq transformer in the input–output synchronous reference frame.

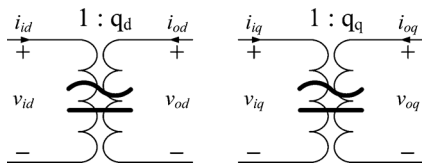


Fig. 4. Matrix converter steady-state and dynamic dq transformer model.

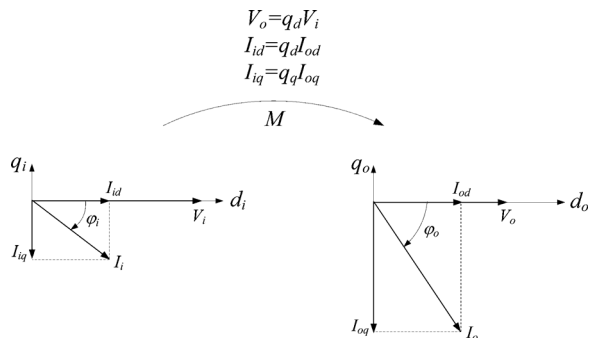


Fig. 5. Modeling of Alesina and Venturini modulation method by the SVD modulation technique.

III. MATRIX CONVERTER REACTIVE POWER CONTROL

Several control strategies based on different modulation techniques can be used to control the input reactive current and power of a matrix converter. All modulation techniques can be modeled by the SVD modulation method. Therefore, this method can be used to study the reactive power capability and control of a matrix converter.

According to Fig. 3, the input reactive power of a matrix converter can be written in a general form as [26]

$$\begin{aligned} Q_i &= \Im\{S_i\} = V_{iq}I_{id} - V_{id}I_{iq} \\ &= q_d V_{iq}I_{od} - q_q V_{id}I_{oq} \\ &= Q_{id} + Q_{iq} \end{aligned} \quad (12)$$

where S_i is the input complex power, Q_{id} is the part of the input reactive power made from I_{od} , and Q_{iq} is the part of the input reactive power made from I_{oq} .

Therefore, the following three different strategies of synthesizing the input reactive power of a matrix converter can be investigated:

- Strategy 1: synthesizing from the reactive part of the output current (i.e., Q_{iq});
- Strategy 2: synthesizing from the active part of the output current (i.e., Q_{id});
- Strategy 3: Synthesizing from the active and reactive parts of the output current (i.e., $Q_{id} + Q_{iq}$).

A. Synthesizing From the Reactive Part of the Output Current

If in the SVD modulation technique, θ_i is set to the input voltage phase angle as shown in Fig. 5, the output voltages will also be aligned with the d -axis of the output synchronous reference frame which is defined by θ_o , and the generalized modulation technique will be the same as the Alesina and Venturini modulation technique with a more relaxed limitation on q_d and q_q [24].

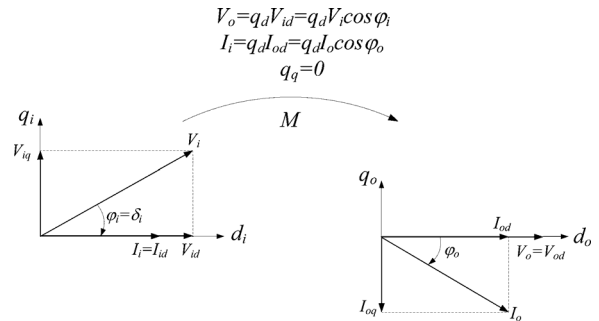


Fig. 6. Modeling the SVM modulation method by the SVD modulation technique.

In this case, q_d controls the voltage gain and q_q controls the reactive current gain of the matrix converter. Therefore, the input reactive power is limited by the voltage gain and the output reactive power as given by (13)

$$\begin{cases} V_o = V_{od} = q_d V_{id} = q_d V_i \\ I_{id} = q_d I_{od} \\ I_{iq} = q_q I_{oq} \end{cases} \Rightarrow \begin{cases} Q_i = Q_{iq} = \frac{q_q}{q_d} Q_o \\ q_d = G_v = \frac{V_o}{V_i} \end{cases} \quad (13)$$

$$(10) \Rightarrow |Q_i| \leq \frac{1 - q_d}{q_d} |Q_o| = \frac{1 - G_v}{G_v} |Q_o| \quad (13)$$

where $G_v = V_o/V_i$ is the voltage gain of the matrix converter and Q_o is the output reactive power.

B. Synthesizing From the Active Part of the Output Current

If q_q is set to zero, as shown in Fig. 6, the output voltage will be aligned with the d -axis of the output reference frame and the input current will be aligned with the d -axis of the input reference frame. Therefore, the SVD modulation technique will be the same as the SVM modulation technique [24].

In this case, q_d controls the voltage gain and ϕ_i controls the input reactive current of the matrix converter. Therefore, the input reactive power is limited by the voltage gain and the output active power as given by

$$\begin{cases} V_o = q_d V_{id} = q_d V_i \cos \phi_i \\ I_i = q_d I_{od} = q_d I_o \cos \phi_o \end{cases} \Rightarrow \begin{cases} Q_i = Q_{id} = V_i I_i \sin \phi_i = P_i \tan \phi_i = P_o \tan \phi_i \\ G_v = q_d \cos \phi_i \leq \frac{\sqrt{3}}{2} \cos \phi_i \Rightarrow \tan \phi_i \leq \frac{\sqrt{\frac{3}{4} - G_v^2}}{G_v} \end{cases} \Rightarrow |Q_i| \leq \frac{\sqrt{\frac{3}{4} - G_v^2}}{G_v} |P_o| \quad (14)$$

where P_o is the output active power.

C. Synthesizing From Both the Active and Reactive Parts of the Output Current

The two previous strategies do not yield the full capability of a matrix converter. To achieve maximum possible input reactive power, both active and reactive parts of the output current can be used to synthesize the input reactive current.

To increase the maximum achievable input reactive current in a matrix converter for a specific output power, its input current

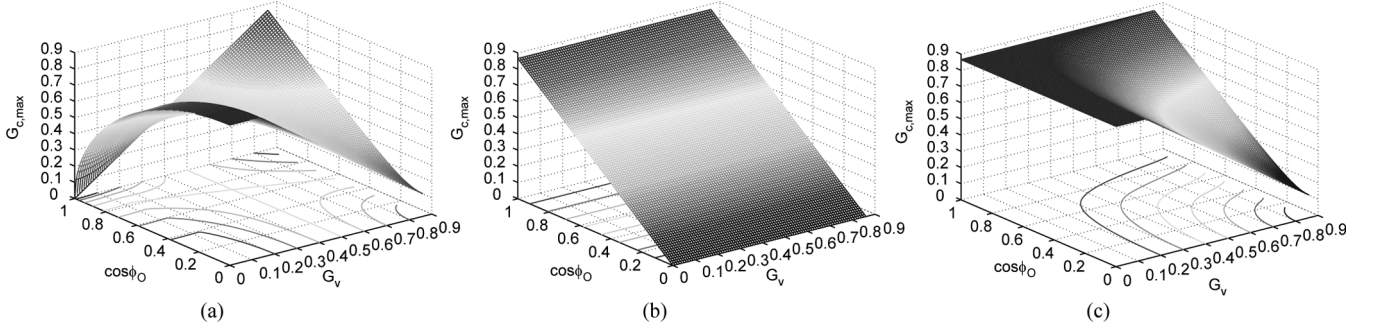


Fig. 7. Maximum achievable current gain of different techniques versus voltage gain and output power factor. (a) Strategy 1. (b) Strategy 2. (c) Strategy 3.

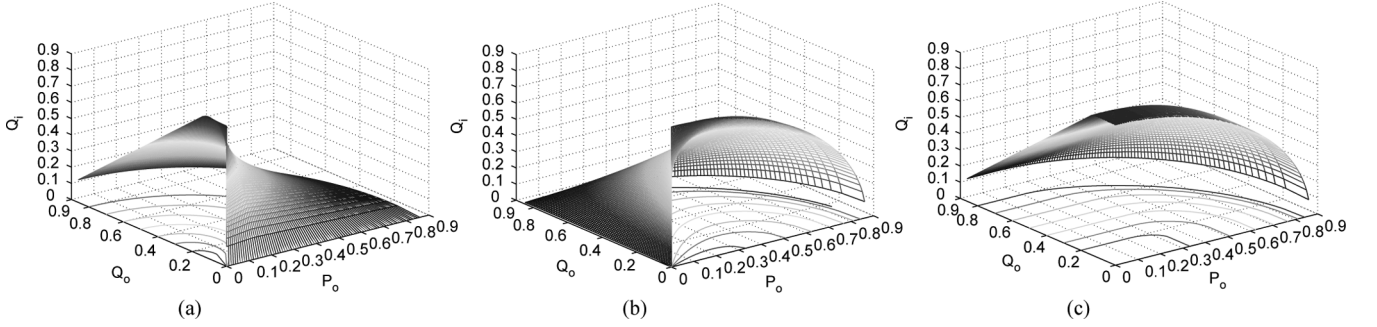


Fig. 8. Maximum input reactive power of different techniques versus output active and reactive power. (a) Strategy 1. (b) Strategy 2. (c) Strategy 3.

should be maximized. Since \mathbf{M}^T transforms I_o from the output space onto the input space, to maximize $|I_i|$, the free parameter θ_i must be chosen such that I_o is located as close as possible to the direction over which the \mathbf{M}^T gain is maximum, i.e.,

$$\max |I_i| = \max_{\mathbf{M}} \{|\mathbf{M}^T I_o|\}$$

$$\text{subject to: } \begin{cases} V_o = \mathbf{M}V_i \\ |q_d|, |q_q| \leq \frac{\sqrt{3}}{2} \\ G_v \leq k = |q_d| + |q_q| \leq 1 \end{cases} \quad (15)$$

where k is a positive parameter which is used to vary the matrix converter constraint. k can be changed from its minimum possible value (i.e., $k = G_v$) to its maximum possible value (i.e., $k = 1$) to change the maximum current gain of the matrix converter (i.e., $G_{c,max}$) and control its input reactive power.

This optimization problem can be solved with different solvers. However, in this section, a closed form formulation is derived to simplify computations of the control system. It is proved in Appendix A that if q_d , q_q , δ_i and δ_o are chosen as given in (16), the input current gain of the matrix converter will be equal to its maximum achievable value for a given parameter k , voltage gain and output power factor

$$\begin{cases} q_d = \min \left\{ k, \frac{\sqrt{3}}{2}, \frac{k + \sqrt{4G_v^2 + k^2 - 4G_v k \sin |\phi_o|}}{2} \right\} \\ q_q = \text{sign}(\phi_i) \text{sign}(\phi_o) \min \left\{ k - q_d, \frac{\sqrt{3}}{2}, \frac{q_d G_v \sin \phi_o}{\sqrt{q_d^2 - G_v^2 \cos^2 \phi_o}} \right\} \\ \delta_i = -\text{sign}(\phi_i) \tan^{-1} \sqrt{\frac{q_d^2 - G_v^2}{G_v^2 - q_d^2}} \\ \delta_o = \tan^{-1} \left\{ \frac{q_d}{q_d} \tan \delta_i \right\}. \end{cases} \quad (16)$$

Figs. 7 and 8 present the maximum current gain and input reactive power in a matrix converter which can be achieved by the three strategies described in this section. As depicted in these figures, the maximum current gain and input reactive power, which can be achieved by the proposed strategy (i.e., strategy 3), are more than that obtained by the other two.

IV. PMS WIND GENERATOR REACTIVE POWER CONTROL

The three methods of controlling the input reactive power of a matrix converter described in the previous section can be used to control the reactive power of a PMS wind generator. A gearless multipole PMS wind generator, which is connected to the output of a matrix converter, is simulated to compare the improvement in the matrix converter input or grid-side reactive power using the proposed strategy. The control block diagram of the system is shown in Fig. 9, and its parameters are listed in Table I. The simulations are performed using PSCAD/EMTDC software.

To control the generator torque and speed, generator quantities are transferred onto the synchronous reference frame such that the rotor flux is aligned with the d -axis of the $dq0$ reference frame. Therefore, I_{gd} will become proportional to the generator torque, and I_{gd} can be varied to control the generator output reactive power. Usually, I_{gd} is set to zero to minimize the generator current and losses. However, in this section, the effect of I_{gd} on the input reactive power is also studied, and a new control structure is proposed which can control the generator reactive power to improve the reactive power capability of the system [27].

A. Fixed I_{gd}

If I_{gd} is set to zero, the generator output current and losses will be minimized. However, since the reactance of a syn-

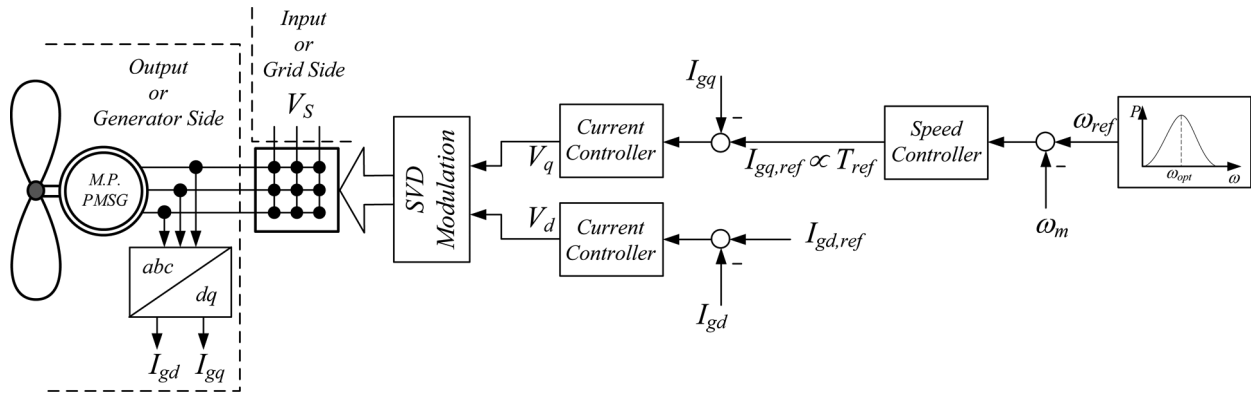
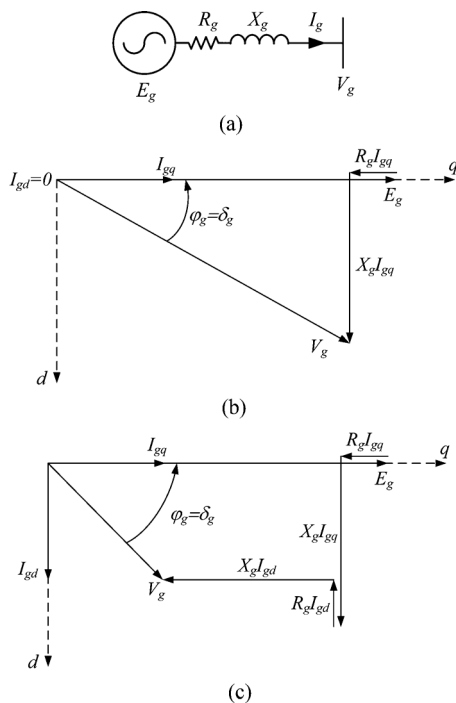


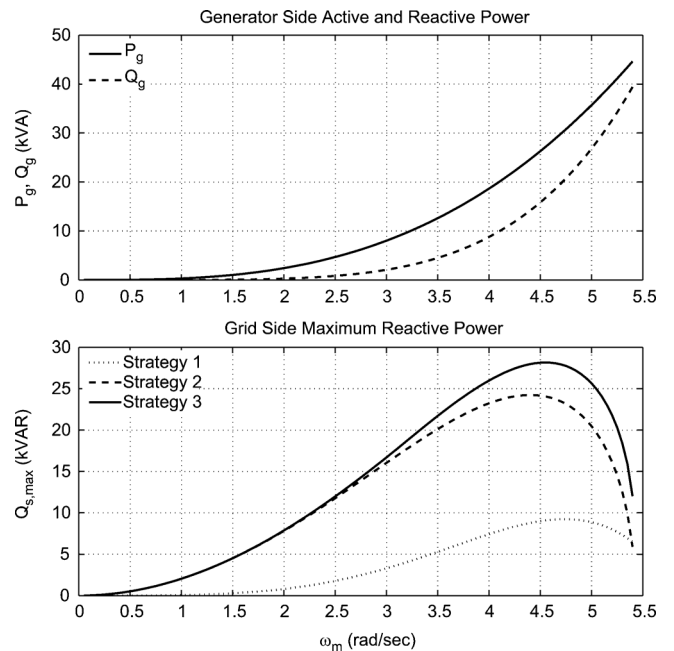
Fig. 9. Simplified control block diagram of a PMSG.

TABLE I
SIMULATED SYSTEM PARAMETERS

Source	V_S	530 V
	f_S	50 Hz
	L_f	0.5 mH
Matrix Converter	C_f	9 μ f
	f_{SW}	10 kHz
	S_g	50 kVA
Generator & Turbine	E_g	380 V
	n_p	58
	f_g	50 Hz
	R_g	0.1 p.u.
	$L_{dg} \approx L_{qg}$	0.8 p.u.
	H_g	1 sec.
	$P_{W,opt}$	$K_{opt}\omega_m^3$
	K_{opt}	314

Fig. 10. Phasor diagram of PMSG for different values of I_{gd} . (a) PMSG equivalent circuit. (b) $I_{gd} = 0$. (c) $I_{gd} > 0$.

chronous generator is typically large, an increase in the wind speed and generator output power leads to an increase in the

Fig. 11. Generator-side active and reactive power and the maximum grid side reactive power versus generator shaft speed ω_m for different strategies.

generator output reactive power. Fig. 10(b) shows a typical phasor diagram of a generator for $I_{gd} = 0$.

Fig. 11 shows the generator active and reactive powers and the maximum grid-side reactive power which can be achieved by the three strategies described in the previous section for different wind speeds and powers. Since an increase in the wind speed leads to an increase in the generator active and reactive powers, the maximum grid-side reactive power, which can be achieved by the proposed strategy, is higher than that obtained by the other two methods.

B. Controlled I_{gd}

Although the maximum achievable grid-side reactive power is improved by the proposed strategy, at low wind speed conditions, the system reactive power capability will be decreased severely which may decrease the system voltage quality and stability. Since, in the proposed strategy, the grid-side reactive current is made from both active and reactive parts of the generator-side current, control of the generator-side reactive power

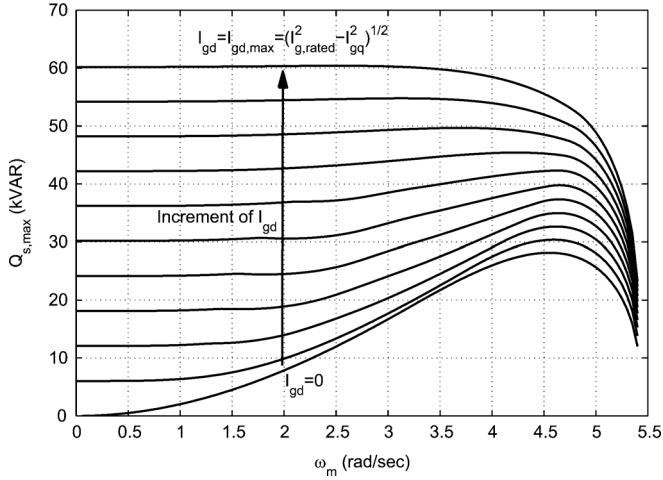


Fig. 12. Grid-side maximum achievable reactive power for different values of I_{gd} .

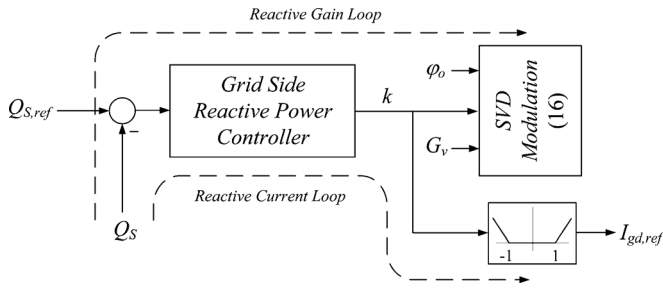


Fig. 13. Proposed control structure which uses I_{gd} and matrix converter synchronously to control the grid-side reactive power.

will be effective in increasing the grid-side reactive power at all wind speed conditions.

As shown in Fig. 10(c), an increase of I_{gd} from zero will increase the generator current and decrease its terminal voltage while its effect on the output active power can be neglected. On the other hand, as depicted in Fig. 7(c), decreasing the matrix converter voltage gain will increase the maximum current gain. Therefore, increasing I_{gd} will increase the grid-side reactive power and improve the system reactive power capability. Fig. 12 shows the maximum achievable grid-side reactive power if I_{gd} is set to a value different from its maximum-allowable value ($I_{gd,max} = \sqrt{I_{g,rated}^2 - I_{gq}^2}$). It can be seen from this figure that if the generator free reactive power capacity is used, a nearly uniform maximum grid-side reactive power can be achieved at all wind speeds.

Since increasing I_{gd} will increase the generator losses, a new control structure is also proposed in Fig. 13 which controls I_{gd} if and only if the maximum grid-side reactive power, which can be achieved for $I_{gd} = 0$, is not sufficient. The proposed structure consists of two reactive gain and reactive current control loops which are controlled by a single reactive power controller. The reactive gain loop controls the matrix converter current gain or ϕ_i by changing the absolute value of parameter k defined in (16). The sign of k defines the sign of ϕ_i or the sign of the grid-side reactive power. When parameter k is lower than its maximum value (i.e., $k = 1$), the reactive current loop, which controls

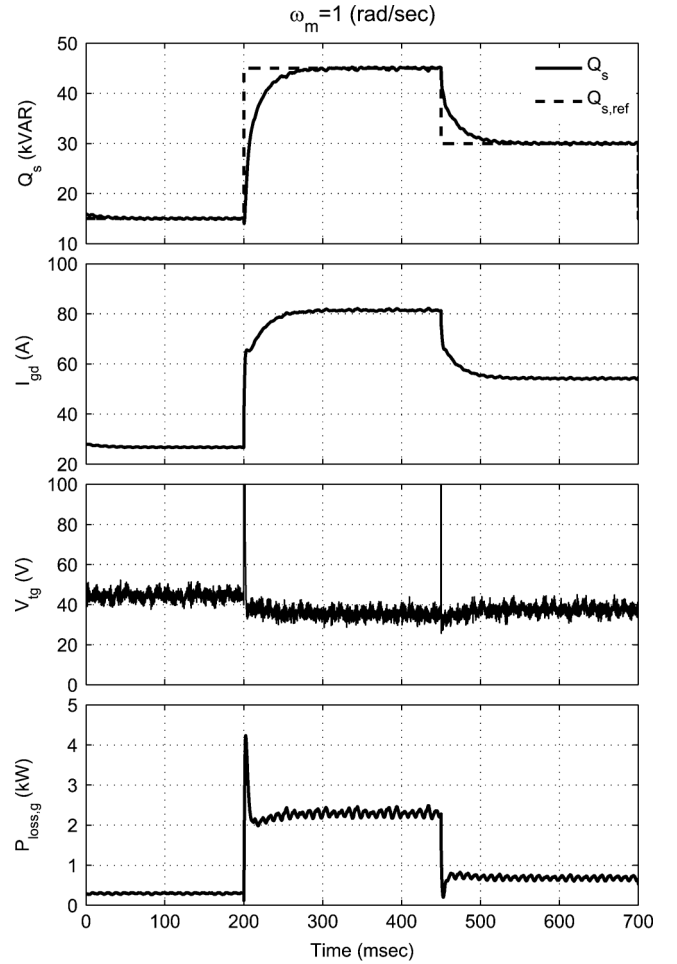


Fig. 14. Matrix converter grid-side reactive power and the generator direct axis current (I_{gd}), terminal voltage and losses for $\omega_m = 1$ rad/s.

$I_{gd,ref}$, is open by the dead zone element, and the reactive gain loop controls the matrix converter current gain. When k reaches its maximum value, the reactive gain loop will be opened due to the saturation of the matrix converter current gain, and the reactive current loop will be controlled by the same controller.

The proposed structure defines $I_{gd,ref}$ in Fig. 9, and G_v and ϕ_o define the desired matrix converter output voltage required to control the generator. This required voltage is generated by the generator current controllers in Fig. 9.

Figs. 14 and 15 depict the simulation results for the proposed control structure for two different generator speeds. The controller used in these simulations for the grid-side reactive power control is a simple adaptive controller (SAC) which is presented in Appendix B. It can be seen from these figures that the controller increases I_{gd} to track the desired grid-side reactive power, if the maximum achievable grid-side reactive power for $I_{gd} = 0$ is not sufficient. An increase in I_{gd} will decrease the generator terminal voltage and increase the generator losses.

V. CONCLUSION

In this paper, a new control strategy is proposed to increase the maximum achievable grid-side reactive power of a matrix converter-fed PMS wind generator. Different methods for controlling a matrix converter input reactive power are investigated.

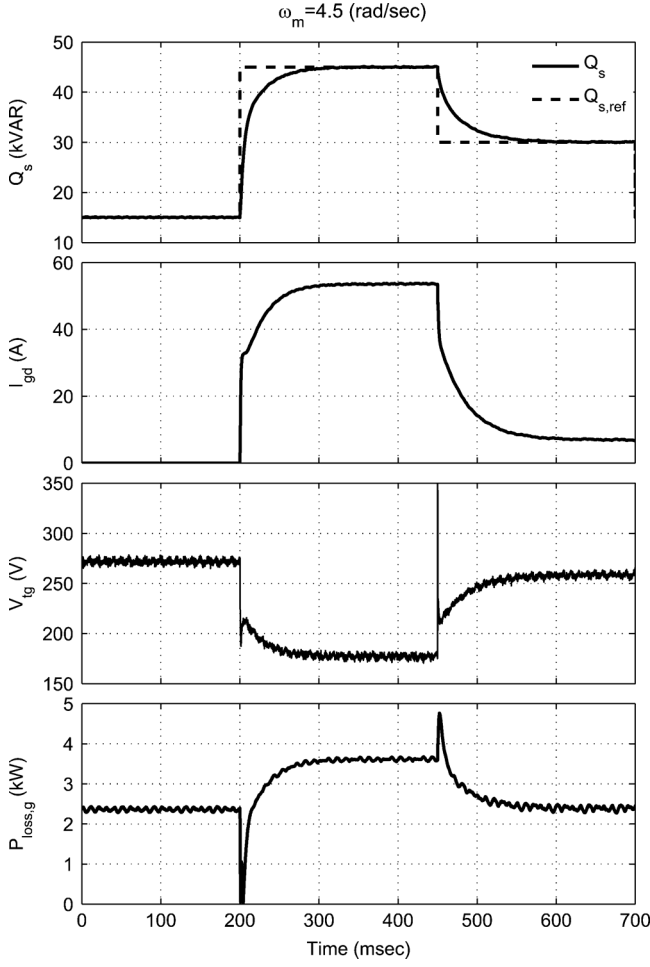


Fig. 15. Matrix converter grid-side reactive power and the generator direct axis current (I_{gd}), terminal voltage, and losses for $\omega_m = 4.5$ rad/s.

It is shown that in some modulation methods, the grid-side reactive current is made from the reactive part of the generator-side current. In other modulation techniques, the grid-side reactive current is made from the active part of the generator-side current. In the proposed method, which is based on a generalized SVD modulation method, the grid-side reactive current is made from both active and reactive parts of the generator-side current.

In existing strategies, a decrease in the generator speed and output active and reactive power, will decrease the grid-side reactive power capability. A new control structure is proposed which uses the free capacity of the generator reactive power to increase the maximum achievable grid-side reactive power. Simulation results for a case study show an increase in the grid-side reactive power at all wind speeds if the proposed method is employed.

APPENDIX A MAXIMUM INPUT CURRENT GAIN

The input current gain of a matrix converter for an specific output voltage and current will be maximum if the input power

factor is minimum or $\tan \phi_i$ is maximum. For this purpose, the following results can be deduced from Fig. 3:

$$G_v^2 = \frac{V_o^2}{V_i^2} = \frac{V_{od}^2 + V_{oq}^2}{V_i^2}$$

$$= q_d^2 \cos^2 \delta_i + q_q^2 \sin^2 \delta_i$$

$$\Rightarrow \tan \delta_i = \pm \sqrt{\frac{q_d^2 - G_v^2}{G_v^2 - q_q^2}} \quad (17)$$

$$\tan \delta_o = \frac{V_{oq}}{V_{od}} = \frac{q_q V_{iq}}{q_d V_{id}}$$

$$= \frac{q_q}{q_d} \tan \delta_i \quad (18)$$

$$\tan(\phi_i + \delta_i) = \frac{I_{iq}}{I_{id}} = \frac{q_q I_{oq}}{q_d I_{od}}$$

$$= \frac{q_q}{q_d} \tan(\phi_o + \delta_o) \quad (19)$$

$\tan \phi_i$ can be obtained as (20) by substituting (17) and (18) into (19)

$$\tan \phi_i = \frac{1}{G_v^2} \left[\mp \sqrt{(q_d^2 - G_v^2)(G_v^2 - q_q^2)} + q_d q_q \tan \phi_o \right] \quad (20)$$

When the SVD modulation dose not reach its constraints (i.e., $q_d \leq \{k, \sqrt{3}/2\}$ and $q_q \leq \{k - q_d, \sqrt{3}/2\}$), the maximum input current and maximum of $\tan \phi_i$ will be achieved if the output current is located on the direction over which the M^T gain is maximum, that is, $\delta_o = -\phi_o$ and $\delta_i = -\phi_i$. Therefore, from (17), q_d and q_q are calculated as follows:

$$\tan \phi_o = \frac{q_q}{q_d} \tan \phi_i = \pm \frac{q_q}{q_d} \sqrt{\frac{q_d^2 - G_v^2}{G_v^2 - q_q^2}} \Rightarrow$$

$$q_q = \pm \frac{q_d G_v \sin \phi_o}{\sqrt{q_d^2 - G_v^2 \cos^2 \phi_o}} \quad (21)$$

However, if the SVD modulation reaches its constraints, q_q can be replaced by $\pm(k - q_d)$ in (20)

$$\tan \phi_i = \frac{1}{G_v^2} \left[\mp \sqrt{(q_d^2 - G_v^2)(G_v^2 - (k - q_d)^2)} \right. \\ \left. \pm q_d (k - q_d) \tan \phi_o \right] \quad (22)$$

Equation (22) concludes that to obtain maximum input current gain, δ_i and q_q must be selected as

$$\begin{cases} \tan \phi_o > 0, \tan \phi_i > 0 \Rightarrow \delta_i < 0, q_q > 0 \\ \tan \phi_o > 0, \tan \phi_i < 0 \Rightarrow \delta_i > 0, q_q < 0 \\ \tan \phi_o < 0, \tan \phi_i > 0 \Rightarrow \delta_i < 0, q_q < 0 \\ \tan \phi_o < 0, \tan \phi_i < 0 \Rightarrow \delta_i > 0, q_q > 0 \end{cases} \quad (23)$$

and q_d be a positive number as

$$\frac{\partial \tan \phi_i}{\partial q_d} = 0$$

$$\Rightarrow q_d = \frac{k + \sqrt{k^2 + 4G_v^2 - 4kG_v \sin |\phi_o|}}{2} \quad (24)$$

Once q_d is obtained from (24), q_q and δ_i can be found from (17), (18), (21), and (23) as follows:

$$\begin{cases} q_d = \min \left\{ k, \frac{\sqrt{3}}{2}, \frac{k + \sqrt{4G_v^2 + k^2 - 4G_v k \sin |\phi_o|}}{2} \right\} \\ q_q = \text{sign}(\phi_i) \text{sign}(\phi_o) \min \left\{ k - q_d, \frac{\sqrt{3}}{2}, \frac{q_d G_v \sin \phi_o}{\sqrt{q_d^2 - G_v^2 \cos^2 \phi_o}} \right\} \\ \delta_i = -\text{sign}(\phi_i) \tan^{-1} \sqrt{\frac{q_d^2 - G_v^2}{G_v^2 - q_d^2}} \\ \delta_o = \tan^{-1} \left\{ \frac{q_q}{q_d} \tan \delta_i \right\}. \end{cases} \quad (25)$$

Changing k results in a variable $\tan \phi_i$ and variable maximum current gain. Equation (25), along with (9), define all required parameters for the SVD modulation to achieve maximum reactive current at the grid side.

APPENDIX B

SIMPLE ADAPTIVE CONTROLLER (SAC)

Most of real plants can be controlled with a simple low-order linear controller. A SAC is somehow a combination of a linear and an adaptive controller which simply guaranties the stability of the system with no difficult constraints [28].

If the state space of an Almost Strictly Positive Real (ASPR) plant is as follows:

$$\begin{cases} \dot{X}_p = \mathbf{A}_p X_p + \mathbf{B}_p u_p \\ y_p = \mathbf{C}_p X_p \end{cases} \quad \mathbf{A}_p \in \mathbb{R}^{n \times n}, \mathbf{B}_p \in \mathbb{R}^{n \times 1}, \mathbf{C}_p \in \mathbb{R}^{1 \times n}. \quad (26)$$

Then, the plant can follow the output of any SISO stable reference model of (27) with the input control law of (28) and the adaptive law of (29).

$$\begin{cases} \dot{X}_m = \mathbf{A}_m X_m + \mathbf{B}_m u_m \\ y_m = \mathbf{C}_m X_m \end{cases} \quad \mathbf{A}_m \in \mathbb{R}^{m \times m}, \mathbf{B}_m \in \mathbb{R}^{m \times 1}, \mathbf{C}_m \in \mathbb{R}^{1 \times m} \quad (27)$$

$$u_p = k_e \underbrace{(y_m - y_p)}_e + \mathbf{k}_x X_m + k_u u_m \quad (28)$$

$$\begin{cases} \dot{k}_e = -\gamma_1 e^2 \\ \dot{\mathbf{k}}_x = -\Gamma_2 X_m^T e \\ \dot{k}_u = -\gamma_3 u_m e \end{cases} \quad (29)$$

where γ_1 , Γ_2 , and γ_3 are the adaptation gains.

The following lemma is useful to obtain an ASPR plant.

Lemma: If G_p is any nonlinear system, and H_c is any stabilizing controller in the form of Fig. 16(a), then the augmented plant of Fig. 16(b) is almost strictly positive real [28].

In this paper, the stabilizing linear controller, reference model, control and adaptive laws are selected as follows:

$$\begin{aligned} H_c &= 0.2 \left(\frac{0.01s + 1}{s} \right) \\ \Rightarrow H_c^{-1} &= \frac{5s}{0.01s + 1} \\ G_m &= \frac{y_m}{u_m} = \frac{1}{0.01s + 1} \end{aligned}$$

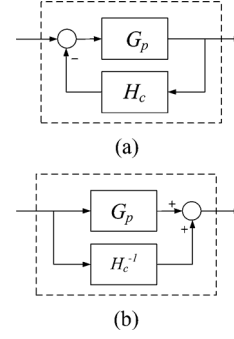


Fig. 16. Almost strictly positive real lemma. (a) Stable structure. (b) Augmented ASPR structure.

$$\begin{aligned} u_p &= k_e \underbrace{(y_m - y_p)}_e + k_x x_m + k_u u_m \\ \gamma_1 &= \gamma_3 = 10^3 \\ \Gamma_2 &= \gamma_2 = 10^3. \end{aligned} \quad (30)$$

The reference model is selected a simple time constant of 0.01, which is larger than the reactive gain and reactive current loops time constants in Fig. 13, and does not pass the second harmonic of the grid-side reactive power. The adaptive gains are chosen by trial and error using simulations in order to achieve a good rate of convergence.

REFERENCES

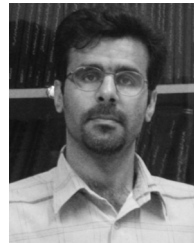
- [1] P. W. Wheeler, J. Rodríguez, J. C. Clare, L. Empringham, and A. Weinstein, "Matrix converters: A technology review," *IEEE Trans. Ind. Electron.*, vol. 49, no. 2, pp. 276–288, Apr. 2002.
- [2] L. Zhang, C. Watthanasarn, and W. Shepherd, "Application of a matrix converter for the power control of a variable-speed wind-turbine driving a doubly-fed induction generator," *Proc. IEEE IECON*, vol. 2, pp. 906–911, Nov. 1997.
- [3] L. Zhang and C. Watthanasarn, "A matrix converter excited doubly-fed induction machine as a wind power generator," in *Proc. Inst. Eng. Technol. Power Electron. Variable Speed Drives Conf.*, Sep. 21–23, 1998, pp. 532–537.
- [4] R. Cárdenas, R. Penal, P. Wheeler, J. Clare, and R. Blasco-Gimenez, "Control of a grid-connected variable speed wecs based on an induction generator fed by a matrix converter," *Proc. Inst. Eng. Technol. PEMD*, pp. 55–59, 2008.
- [5] S. M. Barakati, M. Kazerani, S. Member, and X. Chen, "A new wind turbine generation system based on matrix converter," in *Proc. IEEE Power Eng. Soc. Gen. Meeting*, Jun. 12–16, 2005, vol. 3, pp. 2083–2089.
- [6] M. Chinchilla, S. Arnaltes, and J. C. Burgos, "Control of permanent-magnet generators applied to variable-speed wind-energy systems connected to the grid," *IEEE Trans. Energy Convers.*, vol. 21, no. 1, pp. 130–135, Mar. 2006.
- [7] K. Ghedamsi, D. Aouzellag, and E. M. Berkouk, "Application of matrix converter for variable speed wind turbine driving an doubly fed induction generator," *Proc. SPEEDAM*, pp. 1201–1205, May 2006.
- [8] S. Jia, X. Wang, and K. J. Tseng, "Matrix converters for wind energy systems," in *Proc. IEEE ICIEA*, Nagoya, Japan, May 23–25, 2007, pp. 488–494.
- [9] E. Reyes, R. Pena, R. Cardenas, P. Wheeler, J. Clare, and R. Blasco-Gimenez, "Application of indirect matrix converters to variable speed doubly fed induction generators," *Proc. IEEE Power Electron. Specialists Conf.*, pp. 2698–2703, Jun. 2008.
- [10] R. Vargas, J. Rodríguez, U. Ammann, and P. W. Wheeler, "Predictive current control of an induction machine fed by a matrix converter with reactive power control," *IEEE Trans. Ind. Electron.*, vol. 55, no. 12, pp. 4362–4371, Dec. 2008.

- [11] R. Cárdenas, R. Pena, P. Wheeler, J. Clare, and G. Asher, "Control of the reactive power supplied by a WECS based on an induction generator fed by a matrix converter," *IEEE Trans. Ind. Electron.*, vol. 56, no. 2, pp. 429–438, Feb. 2009.
- [12] V. Kumar, R. R. Joshi, and R. C. Bansal, "Optimal control of matrix-converter-based WECS for performance enhancement and efficiency optimization," *IEEE Trans. Energy Convers.*, vol. 24, no. 1, pp. 264–273, Mar. 2009.
- [13] G. Yang and H. Li, "Application of a matrix converter for PMSG wind turbine generation system," in *Proc. Int. Conf. Clean Elect. Power*, Jun. 9–11, 2009, pp. 619–623.
- [14] S. M. Barakati, M. Kazerani, and J. D. Aplevich, "Maximum power tracking control for a wind turbine system including a matrix converter," *IEEE Trans. Energy Convers.*, vol. 24, no. 3, pp. 705–713, Sep. 2009.
- [15] L. H. Hansen, L. Helle, F. Blaabjerg, E. Ritchie, S. M. Nielsen, H. Bindner, P. Sørensen, and B. Bak-Jensen, "Conceptual survey of generators and power electronics for wind turbines," Risø National Lab., 2001.
- [16] J. A. Baroudi, V. Dinavahi, and A. M. Knight, "A review of power converter topologies for wind generators," *Renew. Energy*, vol. 32, pp. 2369–2385, 2007.
- [17] F. Blaabjerg, Z. Chen, and S. B. Kjaer, "Power electronics as efficient interface in dispersed power generation systems," *IEEE Trans. Power Electron.*, vol. 19, no. 5, pp. 1184–1194, Sep. 2004.
- [18] I. M. de Alegría, J. Andreu, J. L. Martín, P. Ibanez, J. L. Villate, and H. Camblong, "Connection requirements for wind farms: A survey on technical requirements and regulation," *Renew. Sustain. Energy Rev.*, vol. 11, pp. 1858–1872, 2007.
- [19] F. Katiraei, R. Iravani, N. Hatziargyriou, and A. Dimeas, "Microgrids management," *IEEE Power Energy Mag.*, vol. 6, no. 3, pp. 54–65, May/Jun. 2008.
- [20] F. Blaabjerg, R. Teodorescu, M. Liserre, and A. V. Timbus, "Overview of control and grid synchronization for distributed power generation systems," *IEEE Trans. Ind. Electron.*, vol. 53, no. 5, pp. 1398–1409, Oct. 2006.
- [21] A. Alesina and M. G. B. Venturini, "Analysis and design of optimum amplitude nine-switch direct AC-AC converters," *IEEE Trans. Power Electron.*, vol. 4, no. 1, pp. 101–112, Jan. 1989.
- [22] L. Huber and D. Borojevic, "Space vector modulated three-phase to three-phase matrix converter with input power factor correction," *IEEE Trans. Ind. Appl.*, vol. 31, no. 6, pp. 1234–1246, Nov./Dec. 1995.
- [23] D. Casadei, G. Serra, A. Tani, and L. Zarri, "Matrix converter modulation strategies: A new general approach based on space-vector representation of the switch state," *IEEE Trans. Ind. Electron.*, vol. 49, no. 2, pp. 370–381, Apr. 2002.
- [24] H. Hojabri, H. Mokhtari, and L. Chang, "A generalized technique of modeling, analysis and control of a matrix converter using SVD," *IEEE Trans. Ind. Electron.*, vol. 58, no. 3, pp. 949–959, Mar. 2011.
- [25] J. E. Jentle, *Matrix Algebra: Theory, Computations, and Applications in Statistics*. New York: Springer Texts in Statistics, 2007.
- [26] H. Akagi, E. H. Watanabe, and M. Aredes, *Instantaneous Power Theory and Applications to Power Conditioning*. Hoboken, NJ: Wiley, 2007.
- [27] P. Vas, *Sensorless Vector and Direct Torque Control*. New York: Oxford Univ. Press, 1998.
- [28] I. Bar-Kana, "Simple adaptive control—a survey," *Proc. IEEE ICCON*, pp. 257–261, Apr. 1989.



Hossein Hojabri was born in Kerman, Iran, in 1982. He received the B.Sc. degree in electrical engineering from Isfahan University of Technology, Isfahan, Iran, in 2004 and the M.Sc. degree in electrical engineering from Sharif University of Technology, Tehran, Iran, in 2006, where he is currently pursuing the Ph.D. degree in electrical engineering.

His research interests include the application of power electronics in power systems, power quality, and renewable energy systems.



Hossein Mokhtari (M'03) was born in Tehran, Iran, on August 19, 1966. He received the B.Sc. degree in electrical engineering from Tehran University, Tehran, Iran, in 1989, the M.Sc. degree in power electronics from the University of New Brunswick, Fredericton, NB, Canada, in 1994, and the Ph.D. degree in power electronics/power quality from the University of Toronto, Toronto, ON, Canada, in 1999.

From 1989 to 1992, he was with the Consulting Division of Power Systems Dispatching Projects, Electrical Power Research Center Institute. Since 2000, he has been with the Department of Electrical Engineering, Sharif University of Technology, Tehran, Iran, where he is currently a Professor. He is also a Senior Consultant to several utilities and industries. His research interests include power quality, power electronics, and its application in power distribution systems, microgrids, wide-area measurements, and smart grids.



Liuchen Chang (S'87–M'92–SM'99) received the B.S. degree in electrical engineering from Northern Jiaotong University, Beijing, China, in 1982, the M.Sc. degree in electrical engineering from the China Academy of Railway Sciences, Beijing, in 1984, and the Ph.D. degree in electrical engineering from Queen's University, Kingston, ON, Canada, in 1991.

Currently, he is a Professor in the Department of Electrical and Computer Engineering, University of New Brunswick, Fredericton, NB, Canada, where he has been since 1992. He has published more than 200 papers in technical journals and conference proceedings and two books. His principal research interests and experience include distributed generation, renewable energy conversion, power-electronic converters, along with the analysis and design of electrical machines.

Prof. Chang is a recipient of the CanWEA R. J. Templin Award for his research achievements in wind energy technologies. He is a Registered Professional Engineer of APEGNB and a Fellow of the Canadian Academy of Engineering.